ELSEVIER

PII S0142-9612(96)00032-4

Biomaterials 17 (1996) 2037–2044

0142-9612/96/$15.00

Quantitative analysis of fibroblast morphology on microgrooved surfaces with various groove and ridge dimensions

E.T. den Braber*, J.E. de Ruijter*, L.A. Ginsel†, A.F. von Recum‡ and J.A. Jansen*

**University of Nijmegen, Dental School, Laboratory for Biomaterials, POB 9101, 6500 HB Nijmegen, The Netherlands*

†University of Nijmegen, Faculty of Medical Sciences, Department of Cell Biology and Histology, POB 9101, 6500 HB Nijmegen, The Netherlands

‡Clemson University, Department of Bioengineering, College of Engineering and Science, 301 Rhodes Research Center, Clemson, SC 29634-0905, USA

Fibroblasts have been shown to respond to substratum surface roughness. The change in cell size, shape and orientation of rat dermal fibroblasts (RDF) was therefore studied using smooth and microtextured silicone rubber substrata. The microtextured substrata possessed parallel surface microgrooves that ranged in width from 1.0 to 10.0 μm, and were separated by ridges of 1.0 to 10.0 μm. The grooves were either 0.45 or 1.00 μm deep. Prior to incubation, the substrata were cleaned and given a radio frequency glow discharge treatment. After surface evaluation with scanning electron microscopy and confocal laser scanning microscopy, RDF were incubated on these substrata for 5 days. During this period of incubation, the RDF were photographed on days 1, 2, 3, 4, and 5, using phase contrast microscopy. Digital image analysis of these images revealed that on surfaces with a ridge width $\leqslant$4.0 μm, cells were highly orientated (< 10°) and elongated along the surface grooves. Protrusions contacting the ridges specifically could be seen. If the ridge width was larger than 4.0 μm, cellular orientation was random (≈45°) and the shape of the RDF became more circular. Furthermore, results showed that the ridge width is the most important parameter, since varying the groove width and groove depth did not affect the RDF size, shape, nor the angle of cellular orientation. © 1996 Elsevier Science Limited

Keywords: Surface topography, grooves, fibroblast response, quantification, digital image analysis, in vitro

Received 1 August 1995; accepted 25 February 1996

The field of biomaterials is changing slowly. Although biocompatibility is still defined as the ability of a material to perform with an appropriate host response in a specific application[1], recent research has shown that various physicochemical and geometrical material surface properties can be used to modulate the accompanying host response[2–5]. This makes it possible to engineer future biomaterials that provoke a specific biological response, resulting in a unique healing process. Physicochemical properties that have an effect on tissue behaviour are surface charge, surface energy and surface oxidation[5,6]. Geometrical surface properties that can influence the cellular interactions are shape, size and topography of a surface. The latter is not only limited to surface conditions like roughness or curvature, but also includes microtextured surfaces with a standardized surface roughness. For example, *in vitro* experiments have already demonstrated that surfaces possessing microgrooves induce orientation of fibroblasts[3,6,7]. This phenomenon is also known as 'contact guidance'[8]. In two previous studies[6,7], we reported that especially surfaces with a 2.0 μm groove–2.0 μm ridge configuration were able to induce strong orientation and elongation of the fibroblasts cultured on these substrata. Surfaces with 10.0 μm grooves and ridges, however, did orientate the cells. All the grooves of those experiments were 0.45 μm deep. Further, we found that the proliferation rate of the rat dermal fibroblasts cultured on the microtextured surfaces was changed by the wettability of the surface[6], but not by the different topological micro dimensions on the substratum surface[6,7].

Although the influence of microtextured surfaces on the cellular behaviour is evident, very little is known

Correspondence to Dr E.T. den Braber.

about the fundamentals and basic mechanisms of this phenomenon. Several hypotheses have been proposed to explain this specific cellular behaviour. Some investigators suggest that the fibroblasts not only orientate, but also conform to the topography of the biomaterial surface, thus leading to mechanical interlocking[9]. Others[6,7,10,11] argue that cells on microtextured surfaces are able to rearrange their architecture in a three-dimensional orientation and establish an equilibrium of internal and external forces. This could result in a relaxed cytoarchitecture, which favours cellular differentiation.

Considering these theories, it can be questioned whether cells react in a comparable way to surfaces with different geometrical compositions. By varying the groove width, ridge width and groove depth of a standardized parallel groove pattern separately, it will be possible to determine which of these features induces the observed contact guidance. Furthermore, it will be possible to evaluate the impact and importance of the dimensional changes of specific surface features on the cellular behaviour. Therefore, the aim of this study was to quantify the possible changes in fibroblast morphology and orientation after culturing these cells on microgrooved surfaces with various dimensional configurations.

MATERIALS AND METHODS

The substrata

The experimental substrata were produced as described earlier[3,6,12,13]. Briefly, photolithography was used to produce a total of 10 different textured silicon oxide wafers with different surface configurations.

In order to obtain the final experimental substrata, the smooth and grooved silicon oxide wafers were used as moulds, and covered with polydimethylsiloxane (silicone elastomer MDX 4-4210, Dow Corning) to produce a surface replica. After polymerization, the silicone rubber castings were peeled off the moulds and cut into small round discs of 175 mm^2. These substrata were then manually washed in a 10% Liquinox solution (Alconox Inc.), rinsed, ultrasonically cleaned for 30 min in a 1% Liquinox solution, and given two 15-min ultrasonic rinses in distilled, deionized water. Subsequently, they were given a Soxhlet rinse for 12 h in distilled, deionized water. Finally, the substrata were air-dried and prepared for cell culture purposes by radio frequency glow discharge (RFGD) treatment (PDC-3XG, Harrick; Argon, 0.15 Torr, 5 min). After RFGD treatment, the quality and dimensions of the micro features on the substrata were confirmed by scanning electron microscopy (SEM; Jeol 6310) and confocal laser scanning microscopy (CLSM; Zeiss LSM 410).

Cell culture

Rat dermal fibroblasts (RDF) were isolated from ventral skin grafts, taken from male Wistar rats, 40 to 43 days of age (100–120 g). After dissociation, these cells were incubated (37°C, 5% CO_2-95% air) in α-MEM with Earl's Salts and with L-glutamine (Gibco), supplemented with 10% (v/v) heat treated fetal calf serum (Gibco), 2.5 $\mu g\,ml^{-1}$ amphotericin B (Gibco) and 50 $\mu g\,ml^{-1}$ gentamicin (Gibco). After approximately 3 days of culturing the RDF were rinsed with phosphate buffered saline without magnesium and calcium (PBS Dulbecco; pH 7.2), supplemented with 5 $\mu g\,ml^{-1}$ amphotericin B and 100 $\mu g\,ml^{-1}$ gentamicin to remove non-attached cells. Subsequently, the growth medium was added and replaced every two days by fresh growth medium. Upon confluence, the RDF were detached by trypsinization (0.25% (w/v) crude trypsin and 1 mM EDTA (pH 7.2)) and resuspended at a lower cell concentration in fresh growth medium. After identifying the cells as fibroblasts by phase contrast morphology analysis[14], the fifth generation of these cells was used for all experiments.

Substrata with a smooth or microtextured surface were placed in culture wells of 24-well plates (Greiner). After positioning the substrata, the surface grooves were examined with phase contrast microscopy (Leitz DMIL). Subsequently, approximately 1.0×10^4 viable RDF ml^{-1}, suspended in sterile growth medium, were added to each substratum. RDF cultured in wells containing no substratum served as a control group (CTRL). The cells were incubated on a specific substratum for 5 days (37°C, 5% CO_2–95% air) under static conditions. Growth medium was changed every two days. Every substratum configuration was tested in quadruplicate.

Digital image analysis

The effect of the surface microgeometry on the cellular morphology was quantified by digital image analysis (DIA), as described earlier by den Braber *et al.*[7]. In short, RDF at six evaluation areas were photographed by phase contrast microscopy during incubation on days 1, 2, 3, 4 and 5. The evaluation areas were selected by dividing the substratum surface in 740 possible fields of observation of 584.4 $\mu m \times 412.5\,\mu m$. Each of these fields was given a number, which was entered in a randomization program. Thus, a total of four randomly selected evaluation areas and the field at the centre of each substratum were photographed. Registration of the coordinates of these areas assured that the same areas were observed and photographed during the entire period of incubation.

The phase contrast photographs were scanned digitally (400 dpi × 400 dpi) and analysed with an Acorn R260 computer (RiSC processor), the ArcImage 5 for the HAWK V12 frame grabber software package (Foster Findlay Associates, UK) and additional self programmed software. In-house written routines were used to trace all RDF in each digital phase contrast image and to prepare the resulting data for image analysis with the ArcImage program package. The ArcImage program measured several cell parameters, i.e. the cellular surface area, cellular perimeter, cellular circularity, maximum cell length, cell breadth perpendicular to the maximum length, the angle of cellular orientation relative to the surface grooves and number of pitches spanned by a single cell. A schematic representation of these parameters, except the parameter circularity, is

resulting in a number between 0 and 1. If this equation equals 0, the cell has a perfect linear shape, but when circularity is 1, the cell is shaped as a perfect circle.

After gathering the numerical DIA data, these parameters were analysed using univariate, multiple regression, and the non-parametric Kruskal–Wallis models (SAS, release 6.03, SAS Institute Inc., USA).

some small light diffraction peaks were observed on all the substrata. These artefacts were most prominent on the K substrata (*Figure 2*).

Digital image analysis

Figures 3–7 show representative phase contrast images of the RDF cultured on a smooth substrata and surfaces

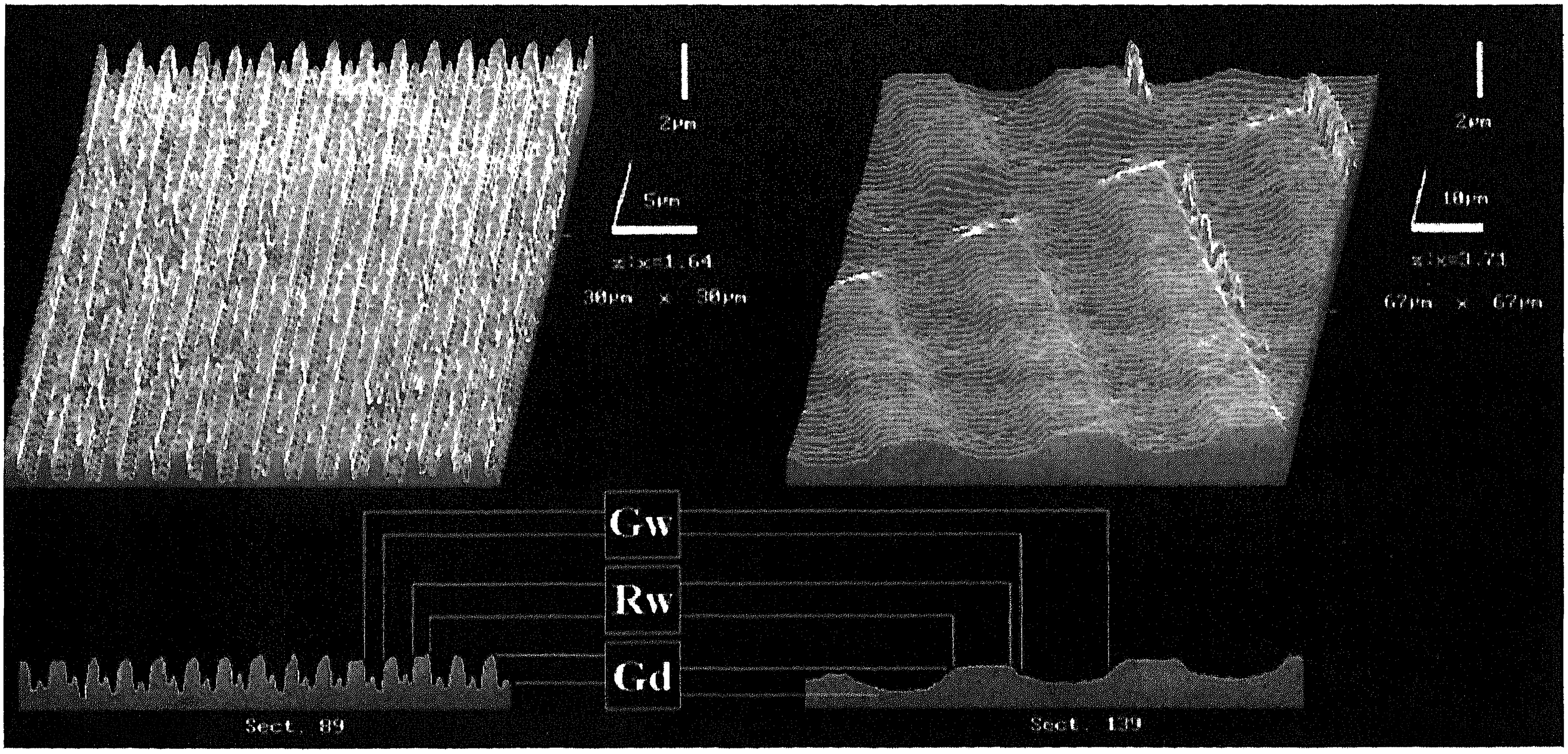

Figure 2 Results of the CLSM surface analysis of a B (left) and a K (right) substratum. Three-dimensional surface representations are given, which are composed out of 256 optical Z sections. Right of the 3D surface profiles the size of the scanned area (30 μm^2 and 67 μm^2 respectively) and difference in X–Y vs Z axis enlargement can be found (1:1.64 and 1:3.71). The codes accompanying the Z sections at the bottom represent the groove width (Gw), the ridge width (Rw) and the groove depth (Gd).

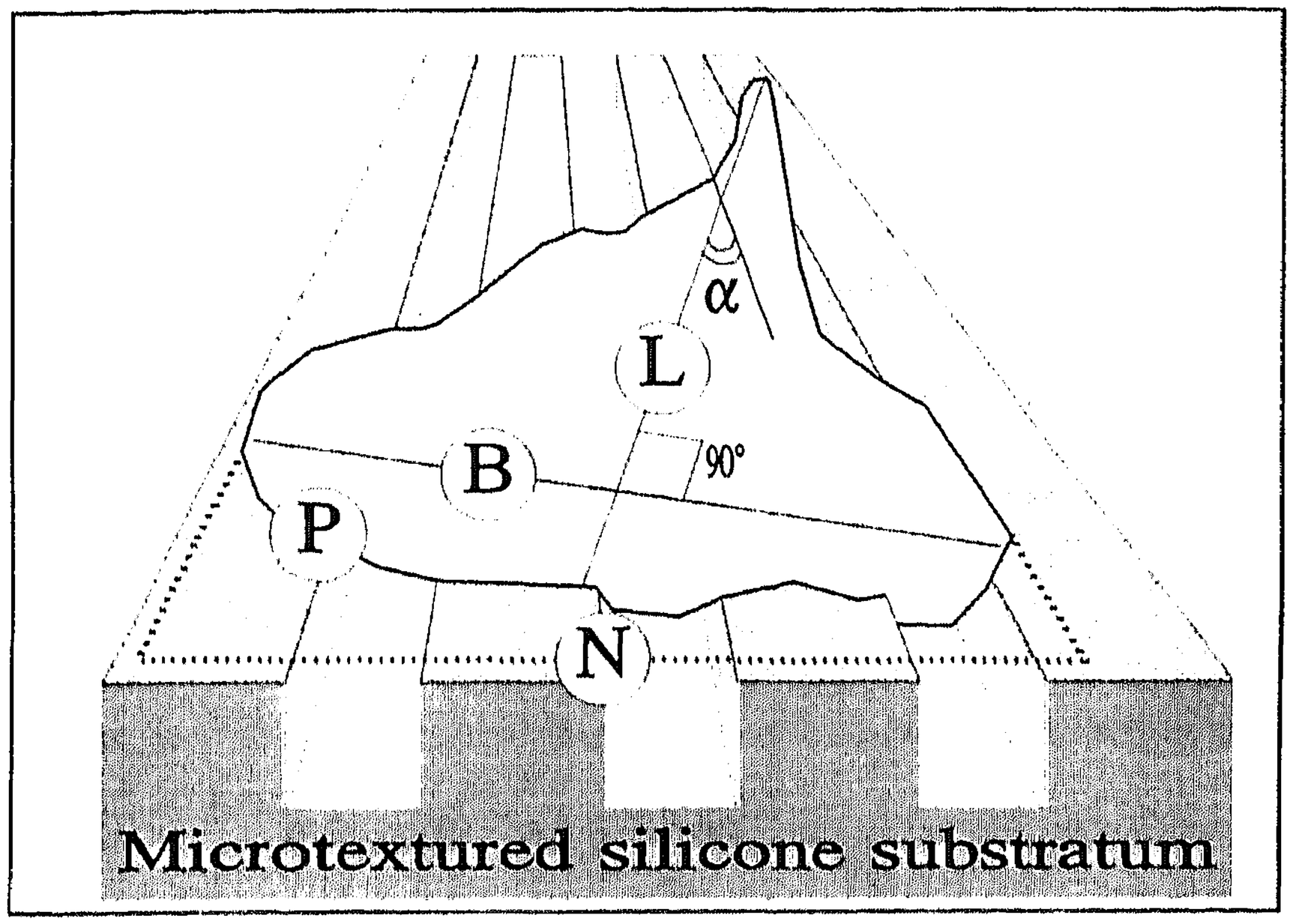

Figure 1 Schematic representation of an RDF on a microtextured substratum. The parameters measured during DIA were the RDF surface area (white area within perimeter), the longest length of the cell (L), the cellular breadth (B), perimeter (P), circularity (not shown), angle of cellular orientation (α) and the number of pitches spanned by the cell (N).

shown in *Figure 1*. Briefly, this parameter is defined as

$$\text{Circularity} = \frac{4\pi\,(\text{Area})}{(\text{Perimeter})^2}$$

Table 1 Dimensions of the micro features on the substrata surfaces (Gd = groove depth, Gw = groove width, Rw = ridge width and P = pitch)

Surface	Gd (μm)	Gw (μm)	Rw (μm)	P (μm)
A	–	–	–	–
B	1.00	1.00	1.00	2.00
C	1.00	1.00	2.00	3.00
D	1.00	1.00	4.00	5.00
E	1.00	1.00	8.00	9.00
F	1.00	4.00	1.00	5.00
G	1.00	8.00	1.00	9.00
H	0.45	2.00	2.00	4.00
J	0.45	5.00	5.00	10.00
K	0.45	10.00	10.00	20.00
CTRL	–	–	–	–

RESULTS

Surface characterization

SEM investigations showed that the parallel grooved surfaces had no defects or irregularities. CLSM measurements demonstrated that the dimensions of the features on the substrata surfaces were well within tolerance levels (*Figure 2*). The dimensions of the specific micro features can be found in *Table 1*. In addition, the optical Z sections showed that the walls of the grooves on the H, J and K substrata were not as steep as on the other microtextured substrata. Also,

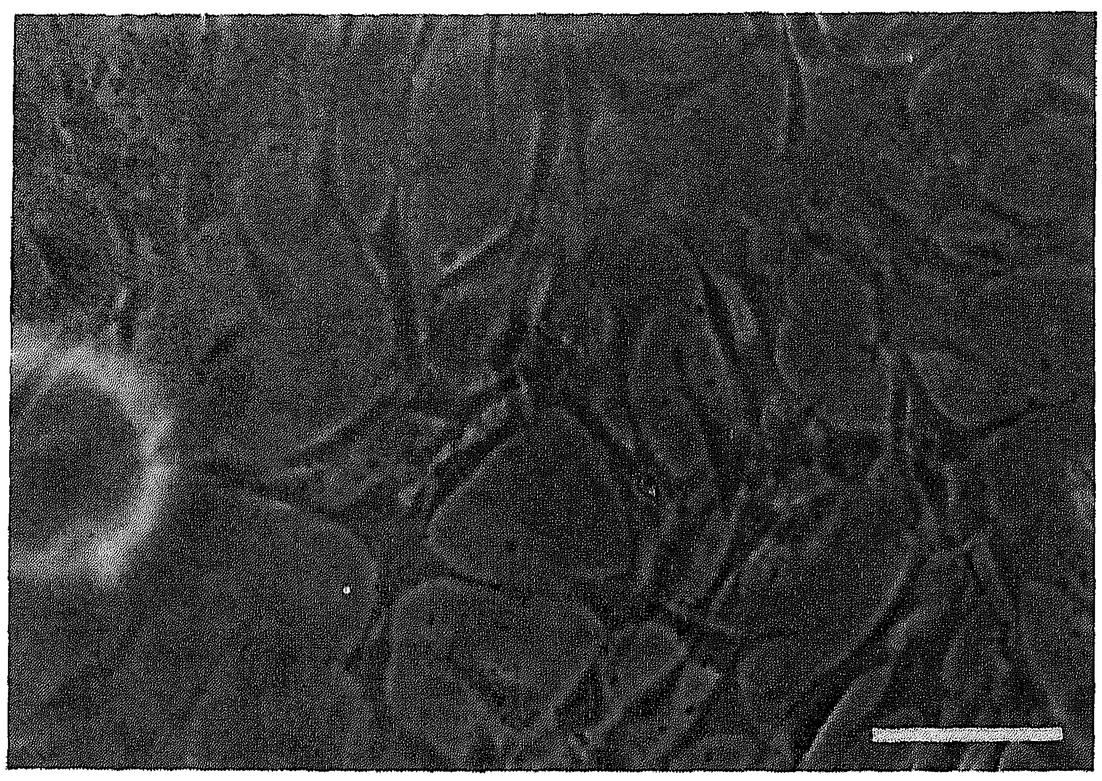

Figure 3 Phase contrast image of RDF on a smooth substratum (A) after 2 days of incubation (bar = 100 μm). The cells are well spread and randomly orientated.

Figure 4 Phase contrast image of RDF on a B substratum (Gw 1.0 μm, Rw 1.0 μm, Gd 1.0 μm, bar 100 μm) on day 1. The cells are highly aligned and elongated along the surface grooves.

with different groove configurations. *Figure 3* shows RDF on a smooth (A) substratum surface. These cells were well spread, multipolar, orientated randomly, and showed a morphology similar to the RDF on the CTRL surfaces (data not shown). Fibroblasts on the grooved substrata showed a wide variety of shapes and angles of orientation relative to the surface grooves. For example, the cells on the B and C substrata appeared to be orientated strongly to the surface grooves. Most of these RDF had a highly elongated spindle shape. RDF on the F, G and H substrata, however, appeared to be orientated along the surface grooves, although these cells were not as highly elongated as those on the B and C surfaces. In contrast, the cellular orientation of the cells on the D, E, J and K surfaces was less clear. Especially orientation of the RDF on the E, J and K substrata did not seem to be affected by the micro features on the substratum surface, while the cells on the D surface appeared to be orientated slightly by the grooves. The shape of the fibroblasts on these last substrata was quite diverse. Spindle shaped, elongated cells could be seen, but spread, multipolar fibroblasts were also present.

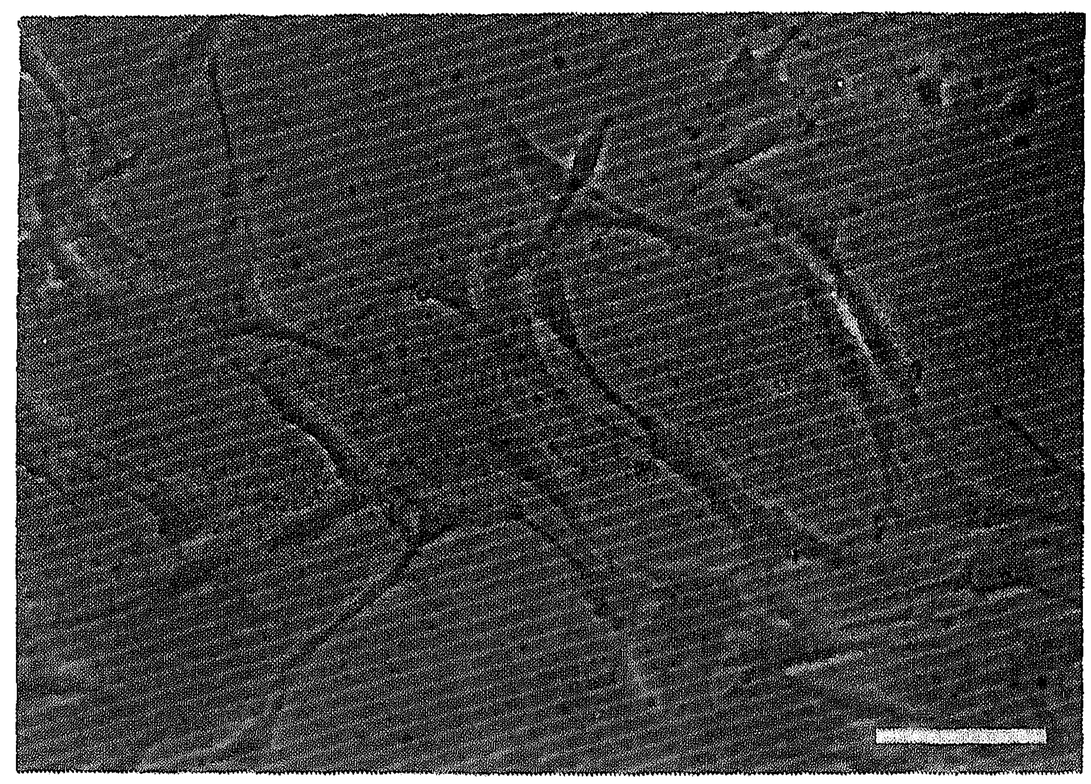

Figure 5 Phase contrast image of RDF on an E substratum (Gw 1.0 μm, Rw 8.0 μm, Gd 1.0 μm, bar 100 μm) on day 2. Spreading and orientation are random.

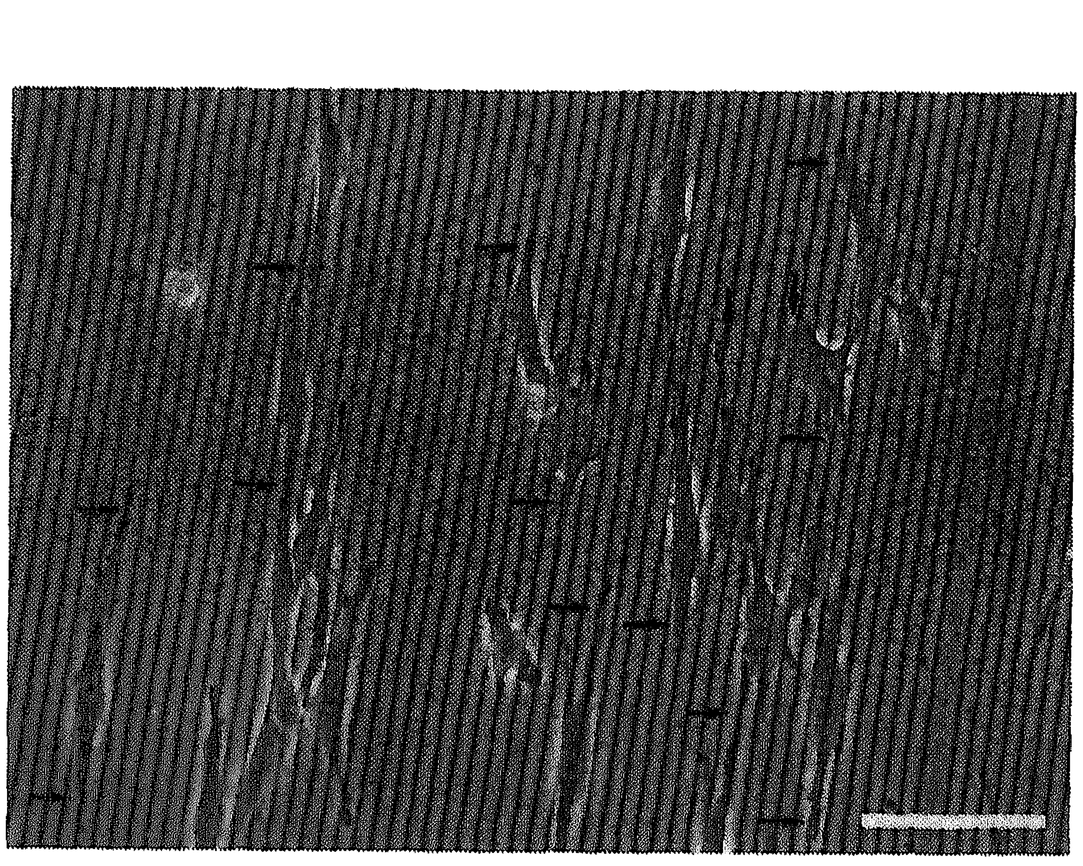

Figure 6 Phase contrast image of RDF on a G substratum (Gw 8.0 μm, Rw 1.0 μm, Gd 1.0 μm, bar 100 μm) on day 1. These substrata are a negative replica of the E substrata (*Figure 5*). Although the cells are not as elongated as on the B (*Figure 4*) substrata, they are clearly orientated. Cell protrusions attach to the ridges (←).

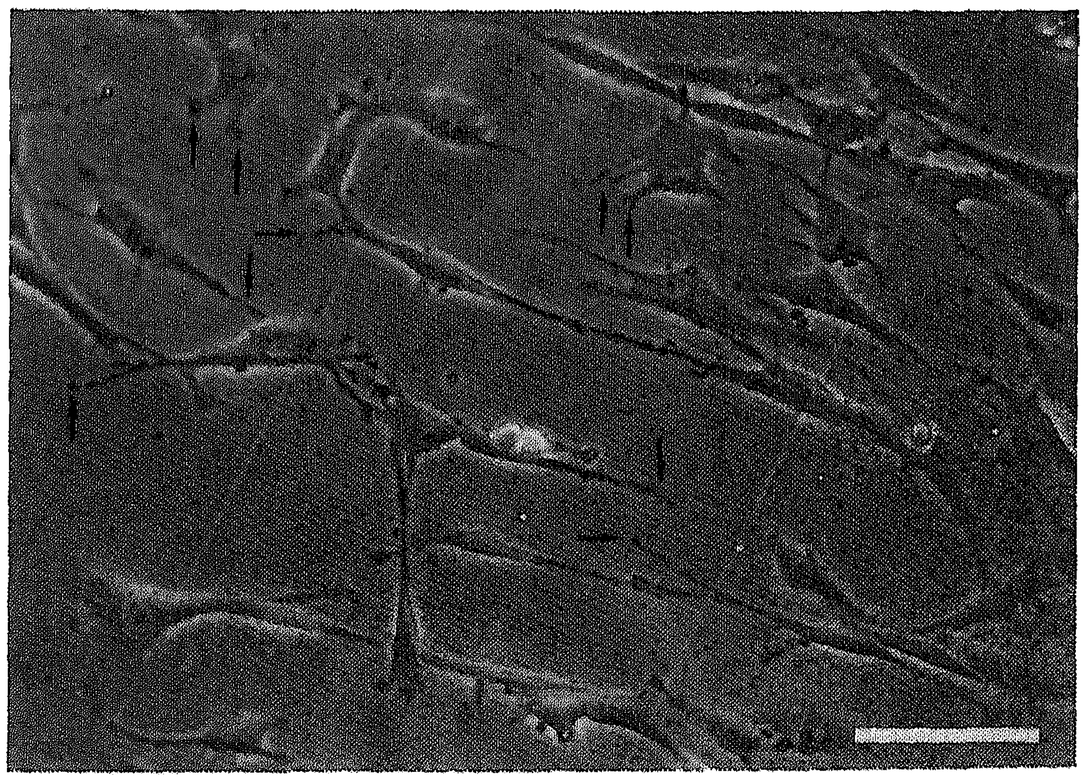

Figure 7 Phase contrast image of RDF on an H substratum (Gw 2.0 μm, Rw 2.0 μm, Gd 0.45 μm, bar 100 μm) on day 1. Elongated, orientated RDF can be seen, although Gd is smaller than on the B–G substrata. Ridge contacting cell protrusions can be seen (←).

Finally, careful examination of the phase contrast images also showed that the cells on the textured surfaces seemed to attach to the ridges of the micropattern. This is best demonstrated by the photographs of the RDF on the G and H substrata (*Figures 6* and *7*). These cells possess several protrusions that end on the (darker coloured) ridges that are situated between grooves (*Figure 2*).

In order to quantify the DIA parameters (*Figure 1*), a total of 5217 cells were traced and evaluated. The quantitative analyses proved that the surface area of the RDF on the B, C and F substrata were significantly smaller ($0.0001 \leqslant P \leqslant 0.0449$) than the cells on the A, E, or CTRL surfaces (*Figure 8*). RDF on the D, G, H, J and K substrata did not show a clear difference in surface area, compared with the cells on the surfaces mentioned earlier. For example, the surface area of the RDF on the G substrata was significantly smaller ($0.0001 \leqslant P \leqslant 0.0127$) on days 1 to 3 than the area of the cells on the A, E and CTRL surfaces. The area of the cells on the G, and the B and C substrata did not differ significantly. However, on days 4 and 5 the opposite was found, since the area of the RDF on the G, B and C substrata did differ significantly, ($0.001 \leqslant P \leqslant 0.0263$), while the cells on the G, A, E and CTRL substrata did not.

Concerning the measured perimeter and (maximum) length of the RDF (*Figure 1*) no continuous, strong significant differences were found (data not shown). For the parameter breadth, however (*Figure 9*), it was found that the cell breadth of the RDF on the B, C, F and G substrata was significantly smaller ($0.001 \leqslant P \leqslant 0.0117$) than the breadth of the cells on the A, E, K and CTRL surfaces. The plots representing the breadth of the cells on the D, H and J substrata (not shown) were positioned in an area between the cell breadth plots of the A, E, K and CTRL surfaces and the B, C, F and G substrata (*Figure 9*). The breadth of these cells did not differ significantly from the cell breadth plots of the upper (A, E, K, CTRL) or the lower margin (B, C, F, G).

Analysis of the RDF circularity (*Figure 10*) showed that the cells on the A, E and CTRL surfaces were significantly rounder than the cells on the B, C, F and G substrata ($0.001 \leqslant P \leqslant 0.0469$). The plots of the fibroblasts on the D, H, J and K substrata (not shown) could be found in the area between these plots, with the A, E and CTRL plots marking the upper margin, and the B, C, F and G plots representing the lower margin of this area.

DIA also calculated the angle of cellular orientation relative to the surface grooves (α; *Figure 1*). The results of these computations (*Figure 11*) showed that the cells on the B, C, G and H substrata were significantly stronger orientated ($0.001 \leqslant P \leqslant 0.0466$) to the surface grooves than the fibroblasts on the D, E, F, J and K substrata. Orientation of the RDF on the F substrata is more complex. On days 1, 3 and 4 the cellular orientation of these cells was not significantly different compared with the orientation of the RDF on the B, C, G and H substrata ($P \geqslant 0.1213$). On the contrary, the orientation of these cells did differ significantly from the orientation of the RDF on the D, E, J and K substrata on days 1, 2, 4 and 5 ($0.001 \leqslant P \leqslant 0.0122$).

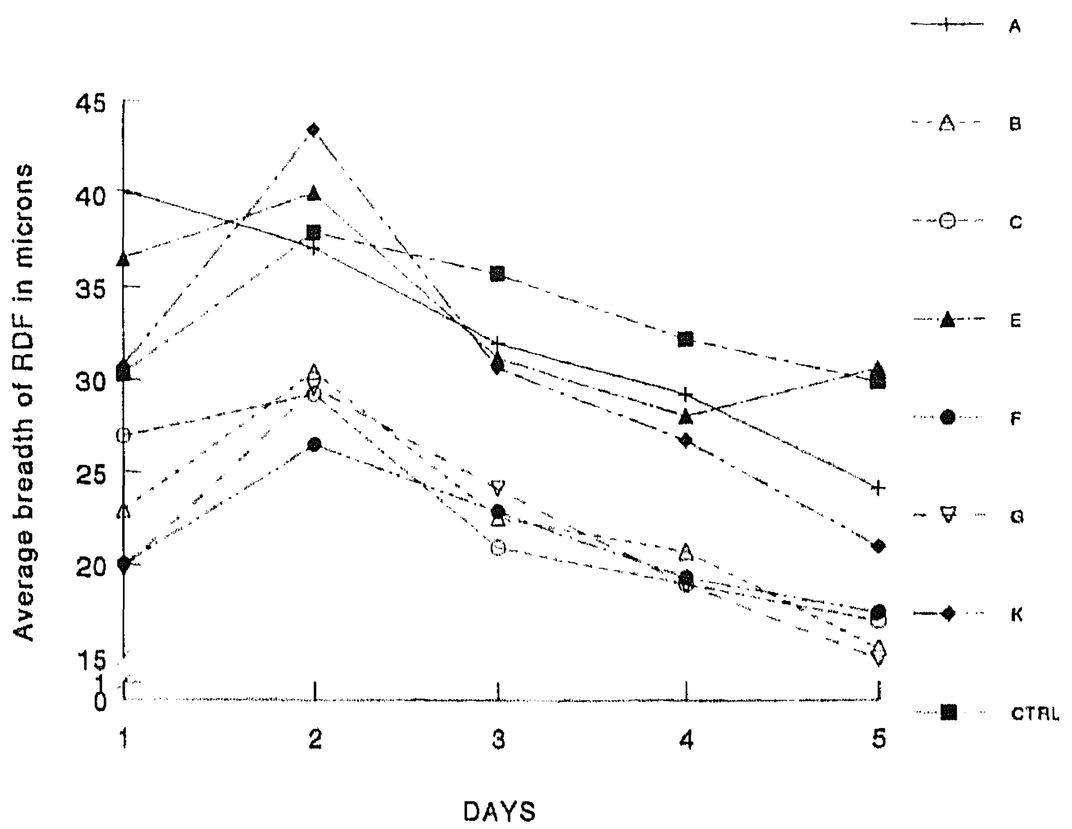

Figure 9 Average cell breadth of the RDF on the various surfaces. The breadth of the RDF on the B, C, F and G substrata is significantly smaller than the breadth of the cells on the A, E, K and CTRL surfaces ($0.0001 \leqslant P \leqslant 0.0117$).

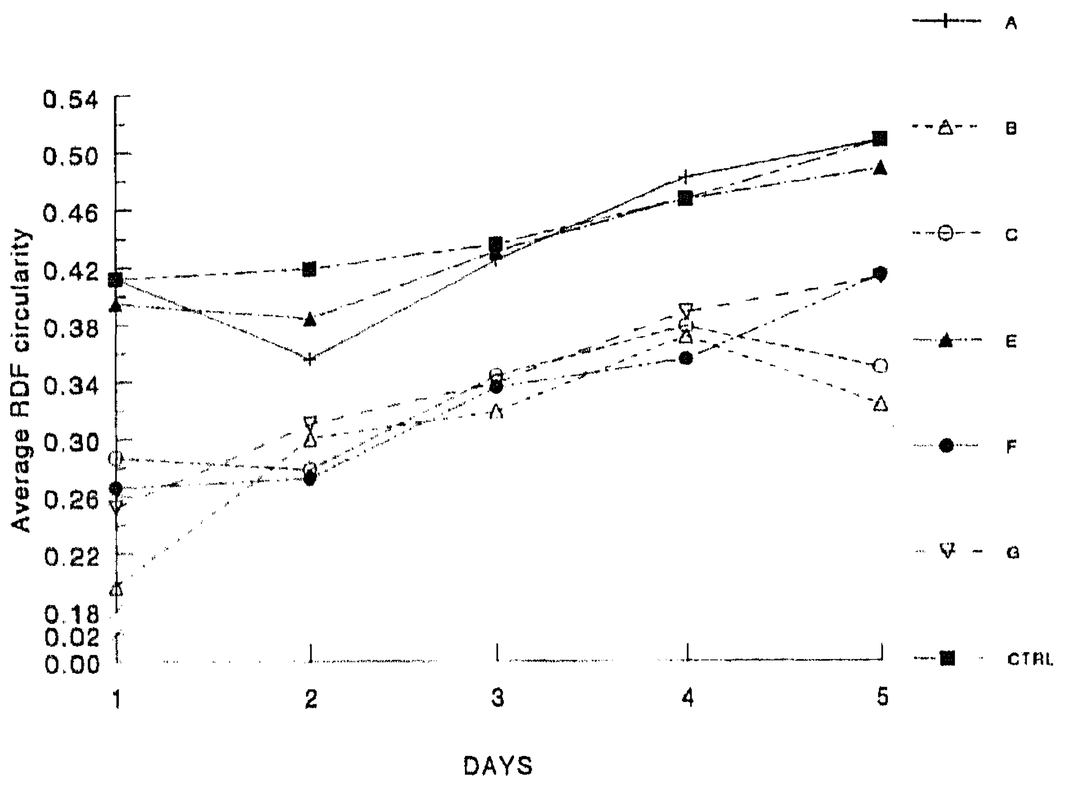

Figure 10 Average circularity of the RDF on the various surfaces. The cells on the A, E and CTRL surfaces are rounder than the RDF on the B, C, F and G substrata ($0.0001 \leqslant P \leqslant 0.0469$).

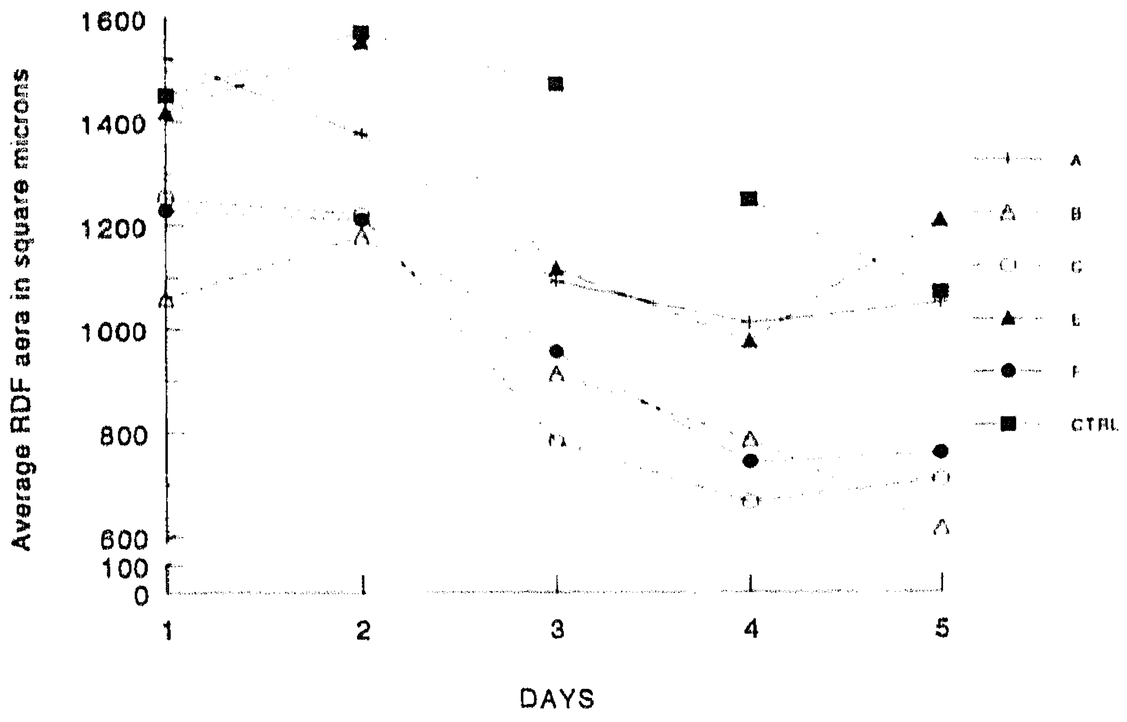

Figure 8 Average RDF surface area on the various surfaces in square microns. The area of RDF on the B, C and F substrata is significantly smaller compared with the area of the A, E and CTRL surfaces ($0.001 \leqslant P \leqslant 0.0449$).

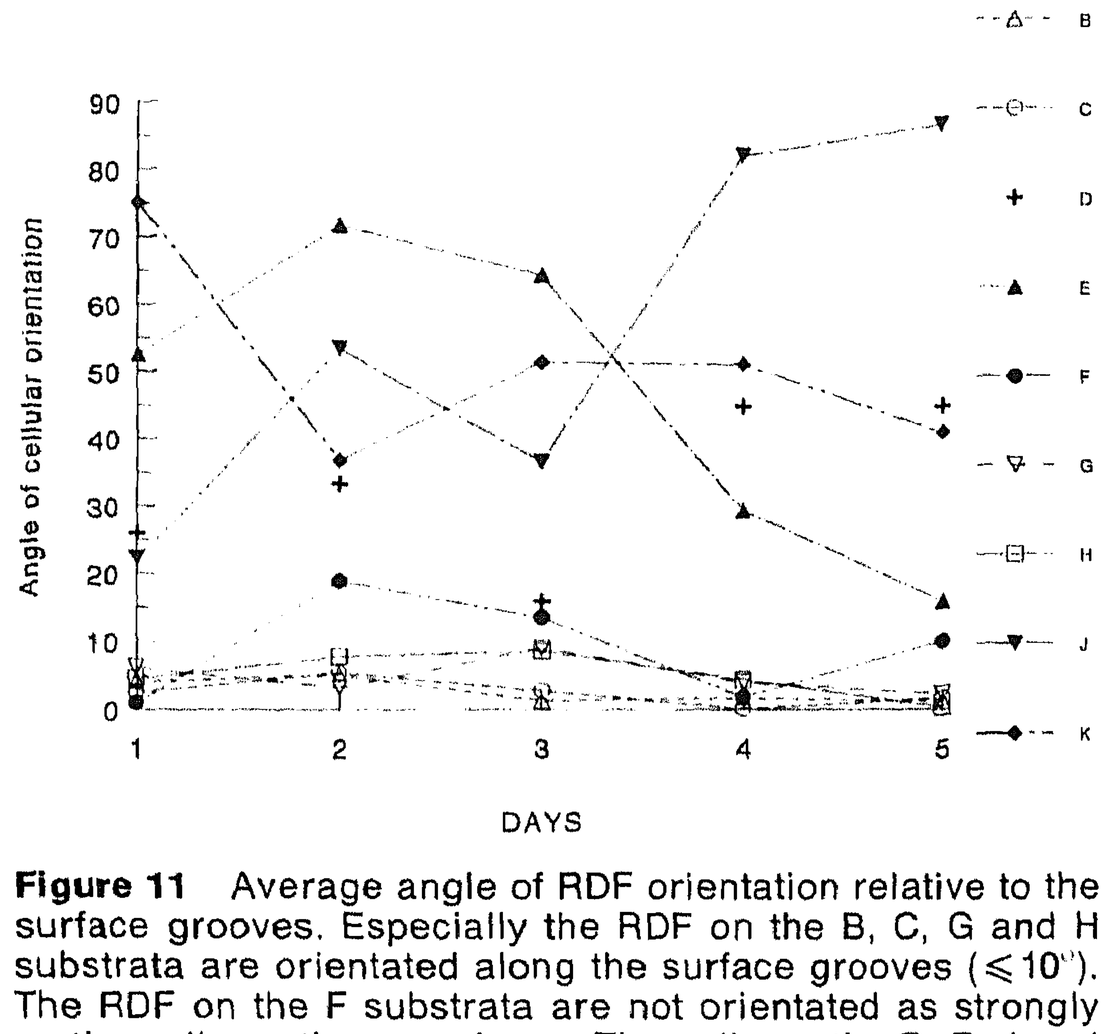

Figure 11 Average angle of RDF orientation relative to the surface grooves. Especially the RDF on the B, C, G and H substrata are orientated along the surface grooves ($\leqslant 10^{\circ}$). The RDF on the F substrata are not orientated as strongly as the cells on these surfaces. The cells on the D, E, J and K substrata clearly have a cellular orientation of $\geqslant 10^{\circ}$.

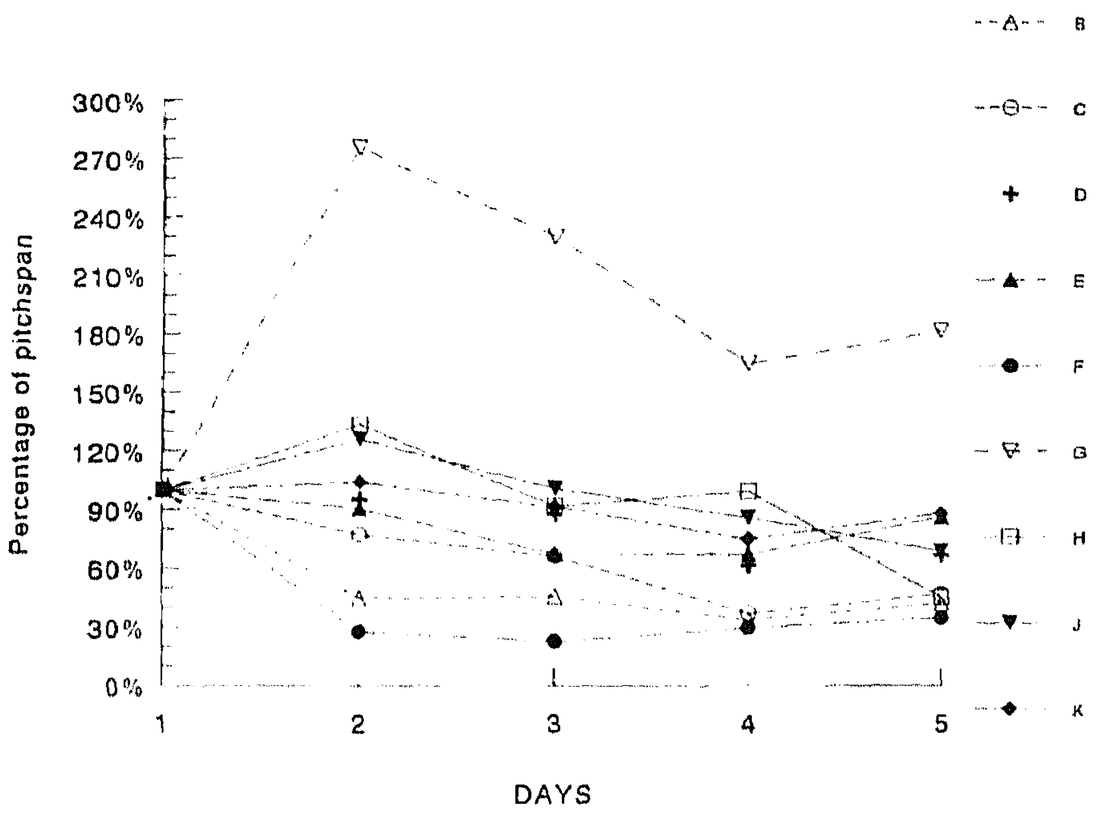

Figure 12 Percentage of RDF pitch span. The total number of pitches spanned on day 1 is defined as 100%. The number of pitches spanned by the RDF is lower on the B and F surfaces than on the C, D, E, G, H, J and K substrata. This is only significant for the cells on the F substrata up to day 3 ($0.0001 \leqslant P \leqslant 0.0369$).

The phase contrast images in *Figure 3–7* also show that the RDF were able to span several grooves and ridges on the textured surfaces. DIA counted the number of pitches spanned by a single cell. On day 1, for example, the RDF on the B, C, D, E, F, G, H, J and K substrata spanned 15.51, 12.66, 6.80, 3.94, 10.36, 1.16, 5.15, 2.30 and 1.89 pitches, respectively. Additionally, the average number of pitches that were spanned by a single RDF on day 1 was defined as 100%, thus making comparison between the different textured surfaces possible. The results of these calculations are shown in *Figure 12*. Although this graph suggests that the number of pitches spanned by the RDF is lower on the B and F surfaces than on the C, D, E, G, H, J and K substrata, statistical evaluation proved that this difference was only significant for the cells on the F substrata up to day 3 ($0.0001 \leqslant P \leqslant 0.0369$). Furthermore, *Figure 12* shows that pitches spanned by the RDF on the G substrata increases on day 2 and remains on a high level. Since the patterns on the D and F substrata, and the E and G substrata were a direct negative replica of each other (*Table 1*), direct statistical testing without a conversion to percentile values was possible. These evaluations showed that up to day 4 the pitch span of the RDF on the F substrata was significantly lower ($0.0001 \leqslant P_{\text{day 1–4}} \leqslant 0.0004$) than on the D surfaces. Furthermore, this procedure showed that the pitch span by the cells was significantly lower ($0.0001 \leqslant P_{\text{day 1–5}} \leqslant 0.0122$) on the E substrata than on the G surfaces.

DISCUSSION AND CONCLUSIONS

Results of this study confirm our earlier findings[6,7] that a microtextured surface can induce orientation of the RDF cultured on these surfaces. DIA and statistical analysis demonstrate that the degree of cellular orientation relates to the dimensions of the micro features on the surface. This becomes even more evident when the alignment criteria that Clark *et al.*[15] suggested are applied to the data plotted in *Figure 11*. These investigators defined a population of cells as highly aligned when the long axis of these cells makes an angle of $<10^{\circ}$ with the direction of the grooves. Review of the data in *Figure 11* shows that the cells on the B, C, G and H substrata, and occasionally on the F surfaces, have an orientation which lies between 0° and 10°. Therefore, these cells have to be considered as highly aligned.

Further review of the DIA results concerning RDF size and shape shows that cells cultured on surfaces with small grooves, and especially small ridges like the B, C and F substrata, have a significantly smaller surface area and cell breadth, while no differences were found in cellular perimeter and length. These findings are supported by the measured parameter circularity, which shows that cells cultured on finely grooved surfaces are less circular than RDF cultured on smooth surfaces. The correlation between these results is quite clear. Since more circular cells possess a cell breadth that is equal or almost equal to the maximum cell length, their area will be larger than the area of the elongated cells which possess a smaller cell breadth. This suggests that the elongated cells on microtextured surfaces change their size by reducing their cell breadth. Although these results are rather straightforward, it is important to note that phase contrast microscopy is a method that results in a two-dimensional picture, not giving any information about the volume of the cell. Therefore, it is possible that the elongated RDF are not as flat as the circular cells. This information could be important in determining whether the elongated cells reduce their size, or just change their shape. Size change would mean that the RDF cultured on microtextured surfaces would actually have a smaller cell volume, where shape change suggests altered cell dimensions by a uniform cell volume. Recent reports by other authors[16] suggest that

optical sectioning with a confocal laser scanning microscope (CLSM) could provide more information on this subject, i.e. cell volume.

Evaluation of the data retrieved during this study also clearly indicates that the width of the ridge is mainly responsible for the contact guidance of the RDF on the microtextured surfaces. This corroborates the findings of Dunn *et al.*[17] and Green *et al.*[18], and is supported by the following results of this study. First, the data plotted in *Figure 11* show that the average angle of cellular orientation (α) of RDF cultured on the B, C, F, G and H substrata is $\leqslant 10°$. The micropatterns on these substrata surfaces possess a ridge width of 1.0, 2.0, 1.0, 1.0 and 2.0 μm respectively, but have different groove width and depth. However, if the ridge is $\geqslant 4.0\,\mu$m, as with the D, E, J and K surfaces (*Figure 11*), α results in an angle larger than 10°, even when the groove width and/or groove depth are identical to these dimensions on the 'orientating' substrata (*Table 1*). Slight orientation ($10° < \alpha < 45°$) can be found with the RDF on the D substrata which possess a ridge width of 4.0 μm. In contrast to this, the cellular orientation on the surfaces with larger ridges like the E, J and K substrata is random, which can be deduced from the fact that $\alpha \approx 45°$. Second, *Figure 11* also demonstrates that the surface parameters groove width and groove depth are considerably less important for RDF orientation than the parameter ridge width. The data plotted in this graph show that the RDF on the B, C, F, G and H substrata are closely orientated along the surface grooves, although the groove width measures 1, 2, 4, 8 and 2 μm, respectively. The same principle applies to the groove depth. Although the H substrata possess grooves of only 0.45 μm deep, no significant differences in RDF orientation were observed, when compared with the B, C, F and G surfaces with 1.0 μm deep grooves. This is in accordance with reports by Dunn *et al.*[17], but differs from results published by Clark *et al.*[15,19], who concluded that groove depth is the most important dimension of parallel grooved substrata influencing the orientation of cells. However, Curtis and Clark[20] also concluded that these effects vary from one cell type to the other. Third, the phase contrast images show that RDF probably attach specifically to the ridges of the surface pattern. This is particularly clear with the RDF on the G (*Figure 6*) and H substrata (*Figure 7*). Careful examination of these photographs reveals that the RDF on these substrata possess cell protrusions that end on, and seem to attach to, the ridges. These possible attachments to the ridges could be associated with surface free energy changes caused by the manufactured, standardized roughness of the substratum surface[21,22]. If the surface energy is more preferable on the ridges, the deposition pattern of the substratum bound attachment proteins will be influenced[23–25]. This could result in the formation of cell–substratum bound contacts primarily on the ridges of the surface micropatterns. The significance of this finding is that surface free energy differences are produced on one and the same material by changing the surface topography. The surface free energy differences in the work of others[23–25] was achieved by differing the surface chemistry. Consequently, the effect of surface free energy and surface chemistry was separated here. This hypothesis is supported by the work of Meyle *et al.*[3], who reported numerous focal adhesion sites on the cellular periphery of gingival fibroblasts that were cultured on silicone surfaces with parallel surface microgrooves. After producing a reflection contrast/fluorescence image by dual channel CLSM, it could be seen that the vinculin positive attachment sites were located on the ridges of the silicone microtextured substratum. Furthermore, Ohara and Buck[26] suggested that focal adhesion plaques are linear structures of 0.25–0.5 μm wide and 2.0–10.0 μm long. Since the geometrical dimensions of these plaques are so specific, only one major orientation of attachment is possible, which is parallel to the surface grooves and ridges (*Figure 13*). Accordingly, a cell attaching to a microtextured surface with small ridges will orientate itself parallel to these ridges. Still, it has to be noted that our results show a decrease of RDF orientation on substrata with a ridge size of $\geqslant 4.0\,\mu$m. This could be explained by the observation of Izzard and Lochner[27] that there is a possible minimum length of 2.0 μm acquired for focal contacts to provide adhesion. Therefore, if the ridge width increases, the possible orientation of adhesion plaque attachment can increase, thus resulting in cell attachment with a larger angle of cellular orientation (*Figure 13*). Finally, reviewing the results of this study, it cannot be excluded that the observed cell–substratum interactions are based on the resemblance of these microtextured surfaces with the topography of the fibrillar extracellular matrix[28], causing the cell to transform and differentiate[5]. If this proves to be true, it is clear that these surfaces could contribute to the process of wound healing around implant surfaces.

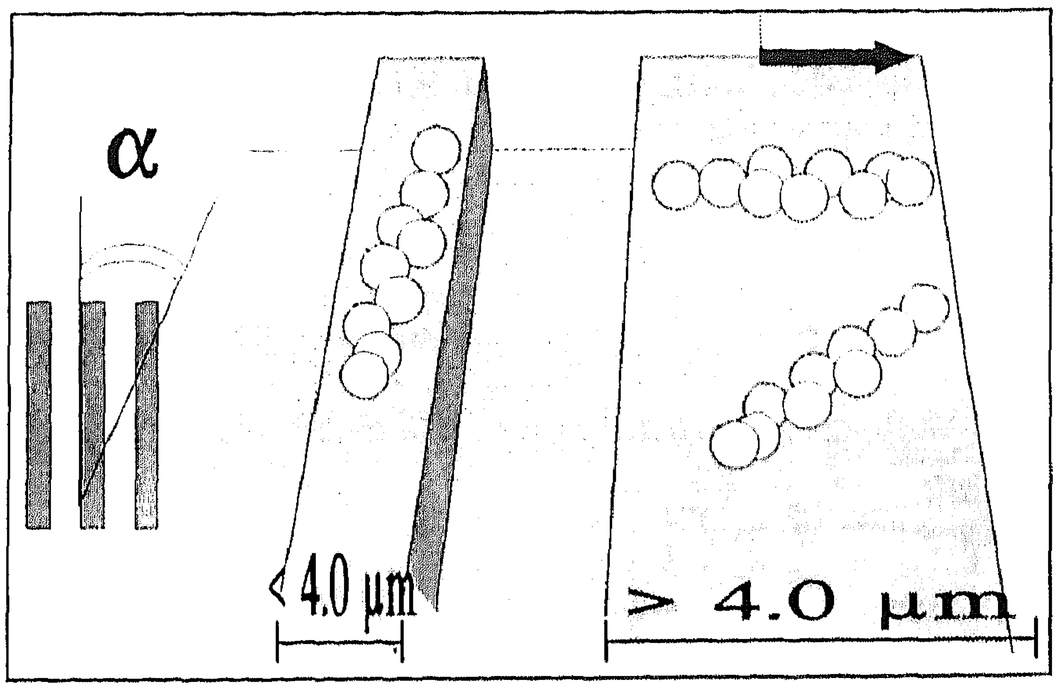

Figure 13 Schematic drawing showing that, on a ridge $< 4.0\,\mu$m, a linear focal adhesion plaque can orientate only parallel to the surface groove/ridge. Hence, $0° < \alpha < 10°$. However, if the ridge width $> 4.0\,\mu$m, the possible angles of orientation (α) increase, resulting in a random cellular orientation ($\alpha \approx 45°$).

ACKNOWLEDGEMENTS

The help of F.A. Scholl (Carl Zeiss, The Netherlands) on the CLSM substratum surface analysis is greatly

appreciated. The authors would also like to thank Dr J. Meyle for the donation of microtextured substrata produced in his laboratories. This study was supported by the Dutch Technology Foundation (STW).

REFERENCES

1 Williams DF. *Definitions in Biomaterials: Progress in Biomedical Engineering*. 4th edn. Elsevier Science: Amsterdam; 1987: 67.

2 Ratner BD. New ideas in biomaterials science–a path to engineered biomaterials. *J Biomed Mater Res* 1993; **27:** 837–850.

3 Meyle J, Gültig K, Brich M, Hämmerle H, Nisch W. Contact guidance of fibroblasts on biomaterial surfaces. *J Mater Sci* 1994; **5:** 463–466.

4 Campbell CE, von Recum AF. Microtopography and soft tissue response. *J Invest Surg* 1989; **2:** 51–74.

5 Singhvi R, Stephanopoulos G, Wang DIC. Review: effects of substratum morphology on cell physiology. *Biotechnology and Bioengineering* 1994; **43:** 764–771.

6 den Braber ET, de Ruijter JE, Smits HTJ, Ginsel LA, von Recum AF, Jansen JA. Effect of parallel surface micro grooves and surface energy on cell growth. *J Biomed Mater Res* 1995; **2:** 511–518.

7 den Braber ET, de Ruijter JE, Smits HTJ, Ginsel LA, von Recum AF, Jansen JA. Quantitative analysis of cell proliferation and orientation on substrata with uniform parallel surface micro grooves. *Biomaterials* 1996; **17:** 1093–1099.

8 Weiss P. Experiments on cell and axon orientation *in vitro*: the role of colloidal exudates in tissue organization. *J Exp Zool* 1945; **100:** 353–386.

9 Meyle J, von Recum AF, Gibbesch B, Hüttemann W, Schlagenhauf U, Schulte W. Fibroblast shape conformation to surface micromorphology. *J Applied Biomat* 1991; **2:** 273–276.

10 Ingber DE. Cellular tensegrity: defining new rules of biological design that govern the cytoskeleton. *J Cell Sci* 1993; **104:** 613–927.

11 Hohn HP, Steih U, Denker HW. A novel artificial substrate for cell culture: effects of substrate flexibility/malleability on cell growth and morphology. *In Vitro Cell Dev Biol* 1995; **31A:** 37–44.

12 Schmidt JA, von Recum AF. Texturing of polymer surfaces at the cellular level. *Biomaterials* 1991; **2:** 385–389.

13 Schmidt JA, von Recum AF. Macrophage response to microtextured silicone. *Biomaterials* 1992; **13:** 1059–1061.

14 Freshney RI. *Culture of Animal Cells; A Manual of Basic Technique*. Alan R. Liss: New York; 1987.

15 Clark P, Connolly P, Curtis ASG, Dow JAT, Wilkinson CDW. Topographical control of cell behaviour: II. Multiple grooved substrata. *Development* 1990; **108:** 635–644.

16 Chehroudi B, Soorany E, Black N, Weston L, Brunette DM. Computer-assisted three-dimensional reconstruction of epithelial cells attached to percutaneous implants. *J Biomed Mater Res* 1995; **29:** 371–379.

17 Dunn G, Brown AF. Alignment of fibroblasts on grooved surfaces described by simple geometric transformation. *J Cell Sci* 1986; **83:** 313–340.

18 Green AM, Jansen JA, von Recum AF. The fibroblast response to microtextured silicone surfaces: texture orientation into or out of the surface. *J Biomed Mater Res* 1994; **28:** 647–653.

19 Clark P, Connolly P, Curtis ASG, Dow JAT, Wilkinson CDW. Topographical control of cell behaviour: I. Simple step cues. *Development* 1987; **99:** 439–448.

20 Curtis ASG, Clark P. The effects of topographic and mechanical properties of materials on cell behaviour. *Critical Reviews in Biocompatibility* 1990; **5:** 343–362.

21 Johnson RE Jr., Dettre RH. Wettability and contact angles. *Surface and Colloid Science*. Vol. 2. Wiley-Interscience: New York; 1969: 85–153.

22 de Jonghe V, Chatain D. Experimental study of wetting hysteresis on surfaces with controlled geometrical and/or chemical defects. *Acta Metall Mater* 1995; **43:** 1505–1515.

23 Baier RE. Surface properties influencing biological adhesion. In: Manly RS, ed. *Adhesion in Biological Systems*. Academic Press: New York; 1970.

24 Schakenraad JM, Busscher HJ, Wildevuur CRH, Arends J. The influence of substratum surface free energy on growth and spreading of human fibroblasts in the presence and absence of serum proteins. *J Biomed Mater Res* 1986; **20:** 773–784.

25 Altankov G, Groth TH. Reorganization of substratum-bound fibronectin on hydrophilic and hydrophobic materials is related to biocompatibility. *J Mater Sci* 1994; **5:** 732–737.

26 Ohara PT, Buck RC. Contact guidance *in vitro*. *Exp Cell Res* 1979; **121:** 235–249.

27 Izzard CS, Lochner LR. Cell-to-substrate contacts in living fibroblasts: an interference reflexion study with an evaluation of the technique. *J Cell Sci* 1976; **21:** 129–159.

28 Clark P, Connolly P, Curtis ASG, Dow JAT, Wilkinson CDW. Cell guidance by ultrafine topography *in vitro*. *J Cell Sci* 1991; **99:** 73–77.